energies

MDPI

Article

Analysis and Mitigation on Switching Transients of Medium-Voltage Low-Harmonic Filter Banks

Joon-Ho Kim [1,2] and Jin-O Kim [1,*]

[1] Department of Electrical Engineering, Hanyang University, Seoul 04763, Korea; comebackjh@hanyang.ac.kr
[2] Hyundai Electric and Energy Systems, Gyeonggi-do 16891, Korea
* Correspondence: jokim@hanyang.ac.kr

Received: 6 April 2020; Accepted: 24 April 2020; Published: 1 May 2020

Abstract: This paper presents the switching transients of medium-voltage low-harmonic filter banks, which have alower back-to-back inrush current and higher transient recovery voltage (TRV) compared with capacitor banks. The switching transients of the filter banks are described by the analytical approach and field measurements for 150 MVA back-to-back filter banks are provided to support the switching phenomena described in this paper. As a mitigation measure of the high transient recovery voltage, a double-breaker type switchgear is analyzed in terms of the operating sequence and the time of the upper and lower breakers. From the analyses, an operation scheme for the double-breaker switchgear is proposed to avoid insulation failure of the breaker during the interruption by mitigating the transient recovery voltage across each breaker.

Keywords: back-to-back inrush current; capacitor switching; harmonic filter banks; switching transients; transient recovery voltage

1. Introduction

Filter banks are applied to mitigate harmonics in power systems by providing a low-impedance path for a certain harmonic frequency [1,2]. Depending on the application and voltage level, there are several types of filter banks, as shown in Figure 1, namely, damping filters for high-voltage direct current (HVDC) systems, detuned filters for low voltage systems, and single-tuned filters for low- and medium-voltage systems [3–5]. A single-tuned filter is the most common filter in industrial applications. It consists of resistance, inductance, and capacitance in series to bypass a certain harmonic to which it is tuned. The configuration and passive components of de-tuned filters are the same as those of single filters. De-tuned filters are used for power factor correction. They also mitigate any harmonics a little bit, and are normally tuned between 4.0 and 4.4.C-type filters have become the most widespread filters among the four types of damped filters, namely: first-order, second-order, third-order, and C-type filters. A C-type filter includes a resistor in parallel to the inductor that produces a damping characteristic at frequencies above the tuning frequency.

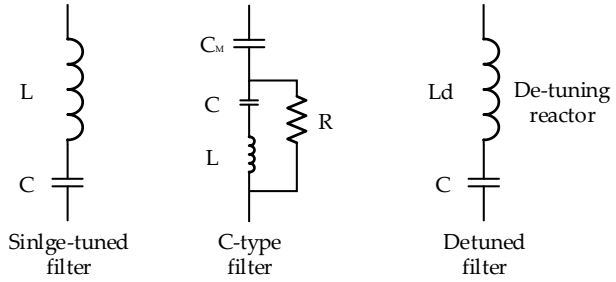

Figure 1. The most widespread passive filter banks in power utilities.

In Korean power grids, one of the representative harmonic loads is an electric arc furnace (EAF) of medium voltage. This load generates lots of power quality issues and has to be integrated into the grid with harmonic filter banks in order to meet the grid code [6–11]. One way widely used for EAFs is to install multiple low-harmonic single-tuned filters for the mitigation of multiple harmonic orders (Figure 2). The EAF system shown in Figure 2 consists of an EAF for steel melting; a thyristor-controlled reactor (TCR) for voltage rise prevention caused by large capacitive filter banks; and four harmonic filters for 2nd, 3rd, 4th, and 5th harmonics mitigation.

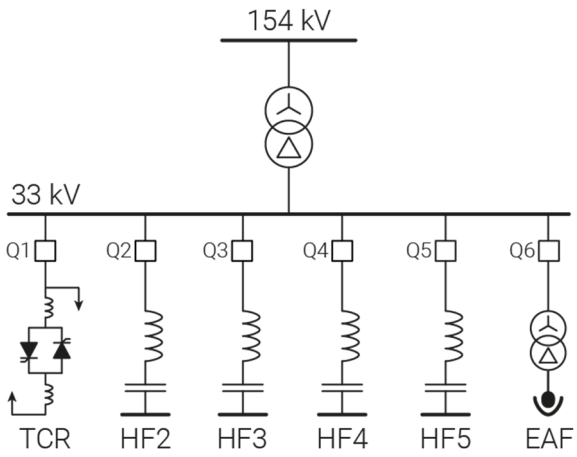

Figure 2. Configuration of an electric arc furnace with four single-tuned filter banks.

Capacitor banks, which are normally used for reactive power compensation, are composed of series and parallel capacitor units. In addition, inductors, often called current limiting reactors, are placed between the main bus and the capacitor banks to mitigate transient inrush currents during the energization, and outrush currents for a short-circuit near to the capacitor banks. The equivalent circuits of the capacitor banks are, therefore, the combination of the inductance and capacitance in series, similar to the single-tuned and de-tuned filters in Figure 1.

A high magnitude and frequency inrush current and voltage occur during back-to-back switching in capacitor banks. Numerous studies have been conducted on how to reduce these switching transient currents and voltages, which can affect equipment damage, system reliability, and power quality [12–25]. The authors of [12] present the considerations that must be given to the phenomenon of the increased transient currents that accompany back-to-back capacitor switching operations and provide references based on industry standards and experiences. The authors of [14] propose installing a surge capacitor across the reactor as well as a standard surge protection package, which can be applied to the existing installations to solve these issues.

While the configuration of both banks is similar, the switching transients between them are completely different because of the different ranges of the inductance value. For capacitor banks, the value of the current limiting reactors is typically several hundred microhenries. On the other hand, harmonic filter banks normally include a higher inductance than capacitor banks, and the inductance value is determined by the system voltage, power frequency, effective reactive power, and tuning harmonic order [26]. Low harmonic filter banks normally include a higher inductance than capacitor banks, which is about several tens of millihenries, especially at a medium voltage [26]. As these characteristics affect transient phenomena, the capacitor bank and the harmonic filter bank must be distinguished and analyzed.

As capacitor banks and filter banks have different characteristics, it should be applied after analyzing the transient study according to each international standard. The standards have not yet been set for the harmonic filter bank, causing problems in designing the back-to-back filter bank. This paper presents the difference between the transient phenomena, which are inrush current, transient voltage, and transient recovery voltage in the back-to-back switching of the capacitor banks and the

harmonic filter banks. To address these problems, an appropriate breaker considering the inrush current and transient voltages due to the back-to-back harmonic filter bank need to be selected and operated. This paper proposes equations to calculate the inrush current, inrush frequency, and transient recovery voltage for the back-to-back switching of harmonic filter banks. Moreover, the mitigation method and operating sequence are presented by an Electromagnetic Transients Program (EMTP) simulation. Transient phenomena, due to the back-to-back switching of capacitor banks and harmonic filter banks, are investigated by field measurements and EMTP simulation. In addition, the proposed mitigation methods are demonstrated through EMTP simulation in a case study.

2. Switching of Filter Banks

The switching of filter banks produces transient voltages and currents. Such phenomena have different characteristics compared with normal capacitor banks, because of the different parameters and/or circuit configurations. Thus, in this section, the peculiarity of single- and de-tuned filter bank switching is discussed with regards to the transient phenomena occurring during energization and de-energization, i.e., transient voltage and inrush current during single and back-to-back filter bank energization, recovery voltage after the current interruption, restrike overvoltage in the recovery phase, and outrush current for the short circuit near to the banks. In this paper, low harmonic filter banks are considered, especially atmedium-voltage. So, it is assumed that the value of the current limiting reactors for the capacitor banks is several hundred microhenries and the value of the current limiting reactors for the filter banks is tens of millihenries.

2.1. Energization of Single Filter Bank

The equivalent circuit of a single bank is a series RLC circuit, as shown Figure 3. It consists of a source, source impedances (R_S and L_S), and filter impedances (L_1 and C_1).

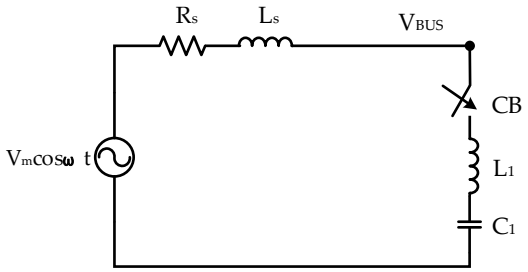

Figure 3. Equivalent circuit for single filter bank energization.

This R–L–C circuit can be written with the single nodal equation. By solving the nodal equation, the natural response for the underdamped condition (inrush current) is as follows:

$$i(t) = V_m \sqrt{\frac{C_1}{L_{eq}}} sin\left(\frac{1}{\sqrt{L_{eq}C_1}}t\right) \tag{1}$$

where $L_{eq} = L_S + L_1$, assuming $R_S = 0$.

The peak and frequency of the inrush current for a single filter bank are the same as those in the literature [27]:

$$i_{peak} = V_m \sqrt{\frac{C_1}{L_{eq}}} \tag{2}$$

and

$$f_{inrush} = \frac{1}{2\pi \sqrt{L_{eq}C_1}} \tag{3}$$

Compared to a capacitor bank, the inrush current and its frequency, associated with single filter bank energization, are greatly reduced by the series tuning reactor. Moreover, the transient overvoltage during energization is also reduced with the reduced inrush current. In other words, neglecting the effects of pre-ignitions, the switchgear may not be stressed with additional over-voltages and inrush currents compared with the regular energizing of a capacitor bank.

2.2. Energization of Back-To-Back Filter Bank

Multiple single-tuned filters are normally employed as a group in order to mitigate multiple harmonic orders. Therefore, multiple single-tuned filters are considered to describe the characteristics of back-to-back filter bank energization.

As the energization of these multiple filters at the same time can result in significant transient overvoltages for low-order harmonic filters, the multiple filters are switched individually [28], known as back-to-back switching conditions [28]. Back-to-back capacitor bank switching occurs when switching C_1 with C_2 for being in service, or vice versa [27]. As shown in Figure 4, the energization of back-to-back filter banks should be started with the filter with the lowest harmonic order, and they should be de-energized from the filter with the highest harmonic filter to the filter with the lowest harmonic filter in order to avoid undesired parallel resonance [28].

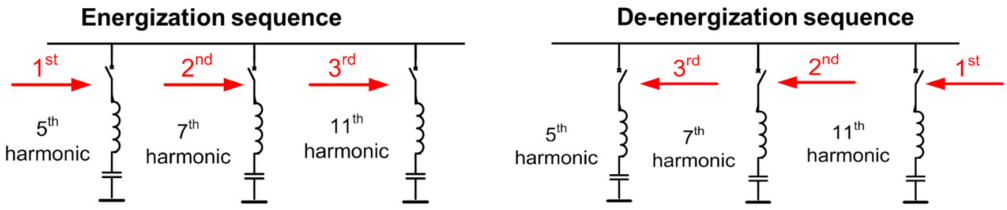

Figure 4. Switching sequence of multiple single-tuned harmonic filters.

The inrush current includes two natural components; one between the bank being energized (C_2 bank in Figure 5) and the bank already energized (C_1 bank in Figure 5), and the other between the source impedance and the bank being energized. If the source inductance, L_S, is much greater than the tuning or current limiting reactors ($L_S \gg L_1$ and L_2), the inrush current is mainly the resonant current between two banks, and it is expressed as follows:

$$i_{2h}(t) = V_m \sqrt{\frac{C_{eq}}{L_{eq}}} sin\left(\frac{1}{\sqrt{C_{eq}L_{eq}}}t\right) \tag{4}$$

where

$$C_{eq} = \frac{C_1 C_2}{C_1 + C_2} \tag{5}$$

and

$$L_{eq} = L_1 + L_2 \tag{6}$$

The peak and frequency of the inrush current for two banks in parallel, which are the same as those in the literature [28], can be written as follows:

$$i_{peak} = V_m \sqrt{\frac{C_{eq}}{L_{eq}}} \tag{7}$$

and

$$f_{inrush} = \frac{1}{2\pi \sqrt{C_{eq}L_{eq}}} \tag{8}$$

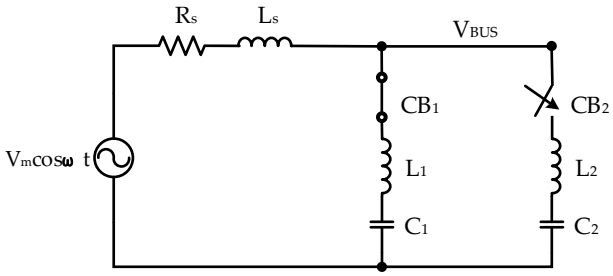

Figure 5. Circuits for back-to-back filter banks energization.

In the case of capacitor banks, the current limiting reactor is sized with relatively small values (approximately several hundred microhenries). Therefore, the resonant current between two banks is dominantly considered, and the above equations are typically used for a capacitor bank application.

On the other hand, if the source inductance, L_S, is much less than the tuning or current limiting reactors ($L_S \ll L_1$ and L_2), the inrush current is mainly the resonant current between the source impedance and the filter bank being energized. It is the same condition for the single bank energization, and its equation is as follows:

$$i_{2h}(t) = V_m \sqrt{\frac{C_2}{L_S + L_2}} sin\left(\frac{1}{\sqrt{C_2(L_S + L_2)}}t\right) \tag{9}$$

From the above equation, the peak and frequency of the inrush current for two back-to-back banks are the following:

$$i_{peak} = V_m \sqrt{\frac{C_2}{L_S + L_2}} \tag{10}$$

and

$$f_{inrush} = \frac{1}{2\pi \sqrt{C_2(L_S + L_2)}} \tag{11}$$

Because of the high tuning reactors of filter banks, the energization of back-to-back filter banks is similar to single bank energization, and the inrush current and its frequency can be calculated by the above equations. Moreover, the transient overvoltage of the back-to-back filter bank energization is also much smaller than that of the back-to-back capacitor bank energization, because the transient overvoltage is associated with the back-to-back inrush current. Table 1 shows the inrush current and transient voltage between back-to-back capacitor banks and back-to back filter banks.

Table 1. Comparing the inrush current and transient voltage between back-to-back capacitor banks and back-to back filter banks.

Contents		Back-To-Back Capacitor Banks	Back-To-Back Filter Banks
Inrush current	Peak	$i_{peak} = V_m \sqrt{\frac{C_{eq}}{L_{eq}}}$	$i_{peak} = V_m \sqrt{\frac{C_2}{L_S+L_2}}$
	Frequency	$f_{inrush} = \frac{1}{2\pi \sqrt{C_{eq}L_{eq}}}$	$f_{inrush} = \frac{1}{2\pi \sqrt{C_2(L_S+L_2)}}$
	Remarks	High inrush current and its frequency supplied by other feeders already energized	Low inrush current and its frequency supplied by the source
Transient voltage	Peak	High	Low
	Dominant frequency	Several frequencies	Power frequency

Thus, it could be summarized that the back-to-back energization of filter banks has a lower back-to-back inrush current magnitude and frequency, as well as lower overvoltage, compared with those of capacitor banks.

2.3. De-Energization of Back-To-Back Filter Bank

Breaking the current of a capacitor bank or a filter bank is like a capacitive switching duty, which is explained first. Afterwards, the differences are pointed out. In the following, a single-phase breaking operation is explained in the circuit diagram given in Figure 6, and the corresponding current/voltage characteristics are also shown in Figure 6. The grid is represented by an AC voltage source, U_s, an inductance L_S, and a capacitance C_s, whereas the load is a simple capacitor, C_l. When the circuit-breaker (CB) opens at time t_0, an arc ignites. Because of the arc characteristics, the current, i_b, is chopped at t_1, prior to the natural current of zero. At this moment, the system voltage, U_s, is nearly at its maximum, because of the capacitive phase angle. In addition, the voltage across the capacitors is higher than the actual source voltage, because of the inductance. This leads to a 1-cos -shaped recovery voltage U_{vac} across the switch with a source side and load side component. The source side transients are caused by oscillations between elements C_s and L_s, which disappear within several milliseconds. At the load side, the capacitor stays charged because no discharge path is available.

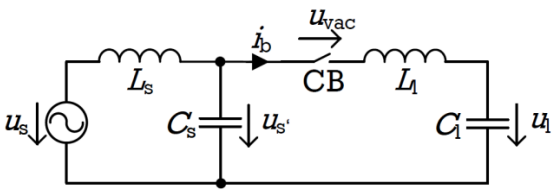

Figure 6. Circuit diagram for single phase filter current interruption.

For a filter bank, the trapped voltage at C_l (U_l) can be calculated as follows:

$$u_l = \frac{Z_{C_l}}{Z_{L_l} + Z_{C_l}} u_{s'} \tag{12}$$

This implies that the trapped capacitor voltage is higher compared with that of a pure capacitor load. In particular, lower harmonic filter banks show a higher trapped voltage, as shown in Table 2.

Table 2. Trapped capacitor voltage for filter banks.

Parameters	Unit	Filter Harmonic Order			
		Second	Third	Fourth	Fifth
System frequency	Hz	50.0	50.0	50.0	50.0
Inductance	mH	56.2	17.6	17.0	9.6
Capacitance	μF	50.0	70.0	40.0	50.0
Trapped capacitor voltage (V_C)	pu	1.38	1.14	1.07	1.05

For medium-voltage applications, filter banks are commonly connected to an ungrounded star connectionto block the flow of the 3rd harmonic current into the system through the grounded neutral. On the other hand, a grounded star connection with the tuning reactor located on the neutral side may be used for high-voltage applications [28]. A delta-connection is only used for a low voltage (e.g., 2400 V) [29], and therefore, this connection was not considered.

The equivalent circuit for the ungrounded filter banks can be drawn as shown in Figure 7. In Figure 7, the ungrounded filter bank is represented by capacitors, C_f, combined with inductors, L_f; while C_{eq} is the capacitance between the circuit breaker (mostly cable capacitance) and the filter bank; and C_n is the capacitance to ground of the neutral.

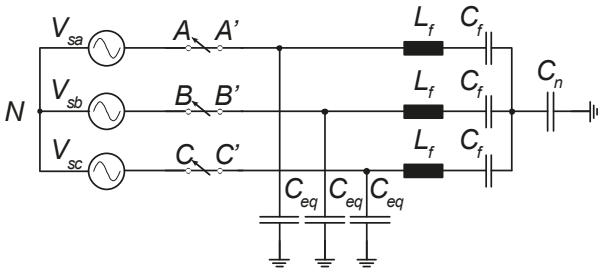

Figure 7. Equivalent circuit for the three-phase filter bank.

Under a steady-state condition, C_n is at the ground potential. When phase A is first interrupted, it makes the three-phase system unbalanced and causes the rise of the potential of the neutral point with half of the trapped capacitor voltage (V_C). If the effect of the inductance is neglected, the transient recovery voltage (TRV) in phase A is the following:

$$V_{AA'} = V_S + 1.5V_C \tag{13}$$

In the case of capacitor banks, the trapped capacitor voltage, V_C, is almost the same as the source voltage, V_S. By assuming $V_C = V_S$, the TRV in phase A of the capacitor banks can reach 2.5 pu (2.5 V_S) [30]. As shown in Table 2, the trapped capacitor voltage, V_C, is higher than the source voltage, V_S, for the filter banks. Therefore, filter banks experience higher TRV than capacitor banks. For example, the TRVs of 2nd and 3rd harmonic filters in Table 2 can reach up to 3.07 pu and 2.71 pu, respectively.

Figure 8 shows the measured transient capacitor voltages during the interruption of the current of a 2nd harmonic filter and the transient recovery voltage of phase A, which is interrupted first; 1 puis equivalent to the source voltage and transient recovery voltage when phase A is interrupted first by EMTP simulation.

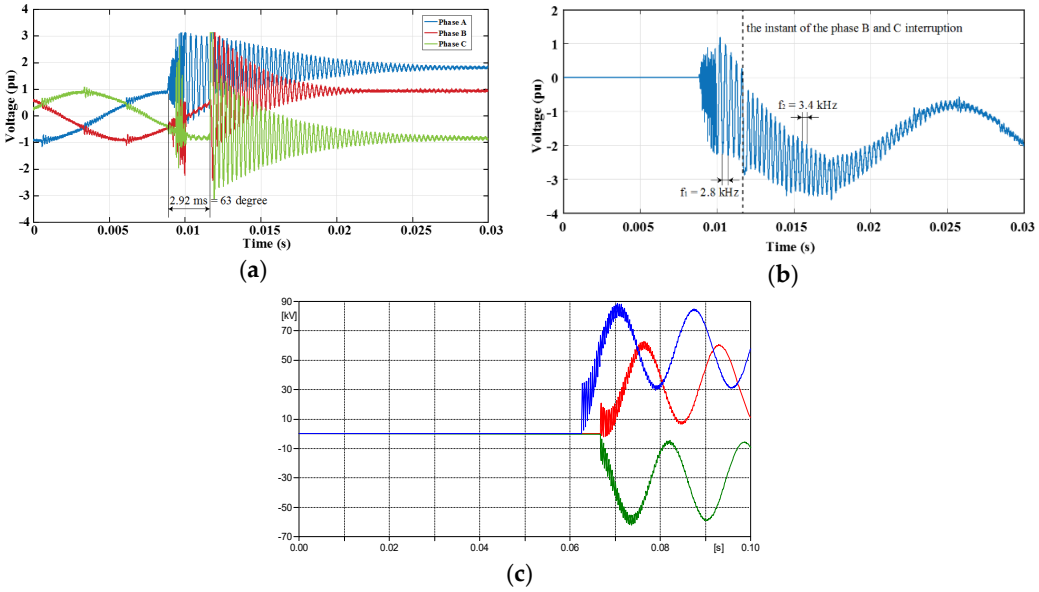

Figure 8. Transient voltages for three-phase filter interruption; (**a**) transient capacitor voltages during the interruption of the 2nd harmonic filter (field measurement); (**b**) transient recovery voltage for phase A interrupted first (field measurement) (**c**) transient recovery voltage for phase A interrupted first (simulation).

Neglecting the pre-ignition, the oscillating capacitor voltage consists of the following two parts: (1) before and (2) after the interruption of phases B and C. Before the interruption of phases B and C,

the transient overvoltage originated from the unbalanced circuit configuration shown in Figure 8a, and its frequency (f_1) can be calculated with the fact that $C_f \gg C_{eq}$ and C_n:

$$f_1 = \frac{1}{2\pi\sqrt{1.5L_fC_{eq}}} \tag{14}$$

The equivalent of the circuit after the interruption is shown in Figure 8b, and its frequency (f_2) is as follows:

$$f_2 = \frac{1}{2\pi\sqrt{L_fC_{eq}}} \tag{15}$$

It is also observed in Figure 9a that after the interruption of phase A, the upcoming current zero-crossing of phases B and C should be a quarter of a cycle (90 degrees) later in the power frequency. However, the interruption of phases B and C happened around 30 degrees earlier than this, around 60 degrees later, because of the harmonics from the thyristor rectifier installed on the same bus with the filter banks.

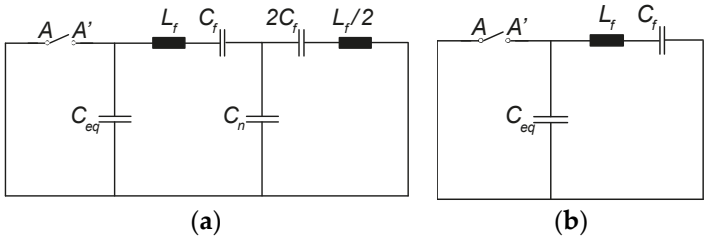

Figure 9. Circuit diagrams for three-phase filter current interruption: (**a**) one phase interruption and (**b**) all three-phase interruption.

The circuit parameters for the measured voltage waveforms in Figure 9 are L_f = 39.1 mH and C_f = 52.5 μF. It is expected that C_{eq} has a very small value, but to know its exact value is difficult in practice. From the measurement, the value of C_{eq} can be calculated reversely as 55 nF, and, with this value, the frequencies of this circuit are the same as the frequencies evaluated from Figure 9b.

For the grounded filter banks, there is no capacitance between the neutral point and the ground. Therefore, the TRV in phase A of the grounded filter banks is smaller than that of the ungrounded case, and its analytical expression is as follows:

$$V_{AA'} = V_S + V_C \tag{16}$$

In addition, the circuit diagram of the ungrounded filter banks is the same as that in Figure 9b for both the 1st phase and all three-phase interruptions, because of their balanced condition. The TRV frequency can be calculated as follows:

$$f = \frac{1}{2\pi\sqrt{L_fC_{eq}}} \tag{17}$$

3. Case Study and Results

A case study was performed to examine the impacts of the switching back-to-back filter banks, which was based on an actual electric arc furnace in South Korea, and aschematic diagram of four multiple single-tuned filter banks is presented in Figure 10. Parameters for thyristor-controlled reactor (TCR) and harmonic filter banks are in Table 3.

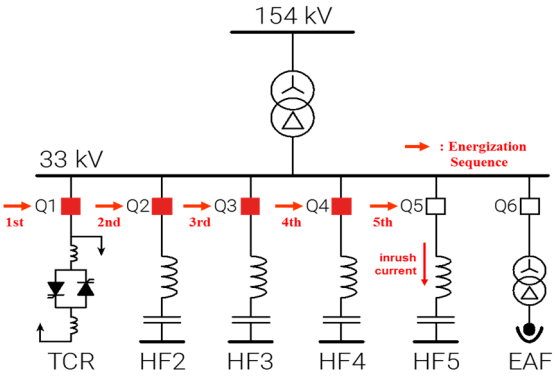

Figure 10. Schematic diagram of four multiple single-tuned filter banks for an electric arc furnace.

Table 3. Parameters for thyristor-controlled reactor (TCR) and harmonic filter banks.

	TCR	HF5	HF4	HF3	HF2
Voltage (kV)			33 kV		
Capacity (MVA)	150	51.4	26.3	42.4	30
Inductance (mH)	19 @ 150 MVA	2.34	7.35	8.7	39.1
Capacitance (μF)	-	122.5	61.3	92.3	52.5
Cable (m)	220	210	225	240	255

A case study was simulated considering three cases, namely (1) the switching of the HF5 with the closed Q1, Q2, Q3, and Q4 CBs; (2) comparing the results considering CB open sequences; and (3) the switching with a double circuit breaker structure in Figure 11, which is EMTP modeling for electric arc furnace.

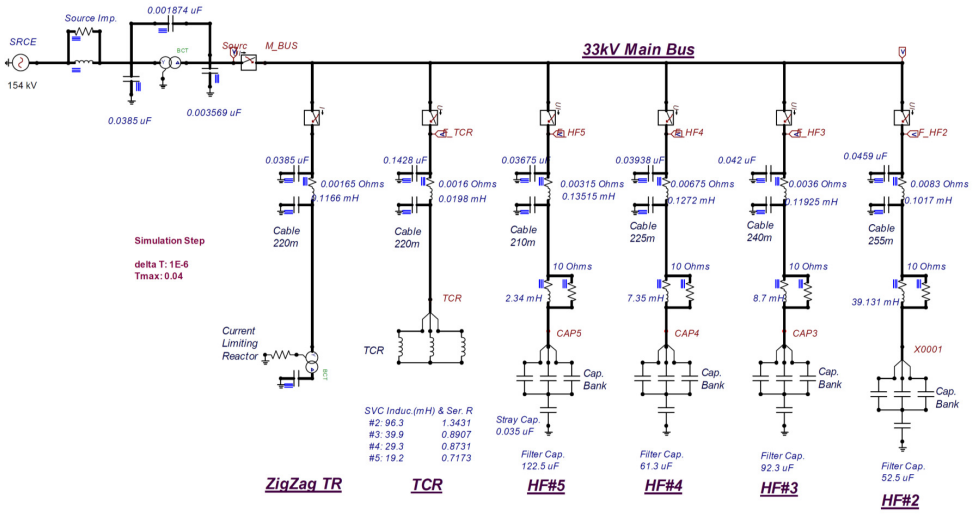

Figure 11. Electromagnetic Transients Program (EMTP) modeling for electric arc furnace.

3.1. Results of Case 1

The inrush current of the back-to-back filter banks with 150 MVA was also presented with its measured waveform so as to discuss the characteristics of the back-to-back filter bank inrush current. The inrush current for the switching of the HF5 was measured under the condition with the closed Q1, Q2, Q3, and Q4 CBs.

The measured current was compared with the EMTP simulation to analyze the inrush current components, as shown in Figure 12. In Figure 12, while there is little deviation between the

two waveforms because of the parameter inequality between the real and simulation circuits, the characteristics in the frequency and the amplitude of the inrush current are almost consistent. With the EMTP simulation, the inrush current contribution of each feeder was analyzed and is compared in Figure 13. The analysis result shows that the inrush current of low harmonic filter banks is mainly the resonant current between the source impedance and the filter bank being energized.

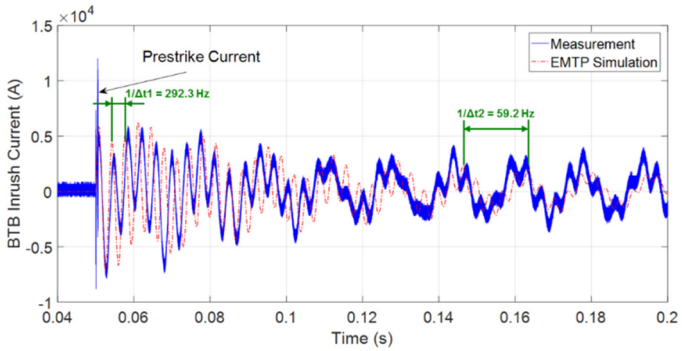

Figure 12. Inrush currents for 5th harmonic filter (HF5) energization.

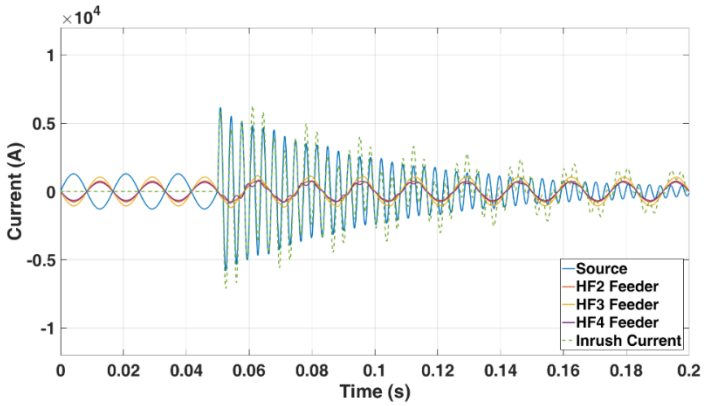

Figure 13. Inrush current and each feeder current for HF5 energization.

3.2. *Results of Case 2*

Initially, all of the breakers were closed, and only the breakers of the corresponding feeders were set to open in 60 ms under individual blocking conditions. In the condition of simultaneous blocking, the main circuit breaker was set to open 10 ms in advance, and the rest of the HF feeders were set to open after 60 ms.

Table 4 shows the results for the transient recovery voltage according to the scenarios, and the waveforms of the simulation of transient recovery voltage are shown in Figure 14. V_S is maximum source voltage, V_L is maximum load voltage, and V_{TRV} is maximum transient recovery voltage of CB.

Table 4. Transient recovery voltage for Case 2.

Condition	CBs	V_S (kV)	V_L (kV)	V_{TRV} (kV)	Waveforms
Individual blocking	HF #2 CB	26.6	61.9	88.5	Figure 14a
	HF #3 CB	26.3	45.8	72.1	Figure 14b
	HF #4 CB	26.6	43.0	69.6	Figure 14c
	HF #5 CB	26.0	42.2	68.2	Figure 14d
Simultaneous blocking	HF #2 CB	0.0	85.2	85.2	Figure 14e
	HF #3 CB	0.0	39.2	39.2	Figure 14f
	HF #4 CB	0.0	35.7	35.7	Figure 14g
	HF #5 CB	0.0	33.7	33.7	Figure 14h

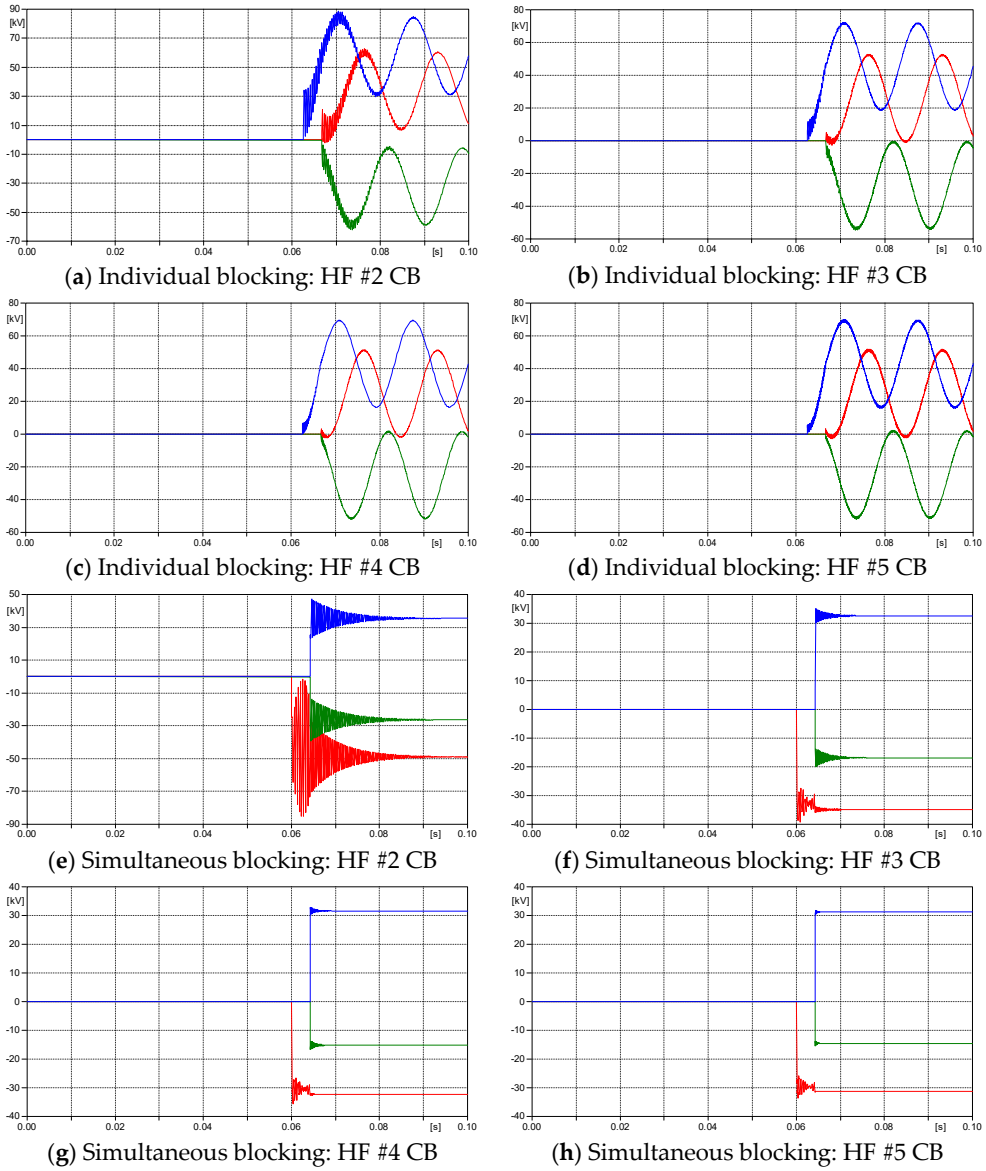

Figure 14. Simulation results of the transient recovery voltage for Case 2.

Under individual blocking conditions, transient recovery voltages up to 88.5 kV are calculated for HF #2 CB. This exceeds the CB test value of approximately 17 kV and may fail to break because of the re-ignition caused by the dielectric breakdown.

In order to reduce the transient recovery voltage without changing the equipment, the circuit breaker operation sequence was changed to the simultaneous blocking condition, but the high transient recovery voltage of 85.2 kV still occurred in HF #2 CB. A very high TRV can occur during the filter bank interruption and it can be one of the severest transients in the filter bank, which might not be a big issue in the capacitor bank interruption. Thus, for the filter bank switching, a higher rating of circuit breakers or circuit breakers with double poles in series is highly recommended to withstand such a high TRV level.

3.3. Results of Case 3: Proposed Method for Reduction Transient Recovery Voltage

The circuit breaker could be damaged because of the transient recovery voltage generated during the breaker operation. In this paper, a switchboard with a double circuit breaker structure is proposed, where two circuit breakers are connected in series to the switchboard, and the breaker damage caused by the transient recovery voltage can be minimized by sharing the transient recovery voltage with the

two circuit breakers. The switchboard consists of a bus vacuum circuit breaker (VCB), which is an upper breaker, and a load VCB, which is a lower breaker.

The transient recovery voltage analysis of each circuit breaker was performed according to the different operating times between the circuit breakers in order to verify the effectiveness of the proposed scheme, and the optimum sequence and operation time. The waveforms of the simulation of the transient recovery voltage are shown in Figure 15, and the results are summarized in Table 5.

If the load VCB is closed after opening the bus VCB, a high TRV may occur in the bus VCB. Additionally, the differences in the breaker open time and the TRV values were not linear. Simultaneous opening of both VCBs and opening the load VCB first, have a high TRV sharing effect that leads to reducing individual breaker TRV. In order to reduce the trapped charge of the load VCB, the two-breaker opening time difference should be kept below 3 ms. In addition, it can share the stress of the VCB operating by controlling the operation sequence of the bus VCB and load VCB.

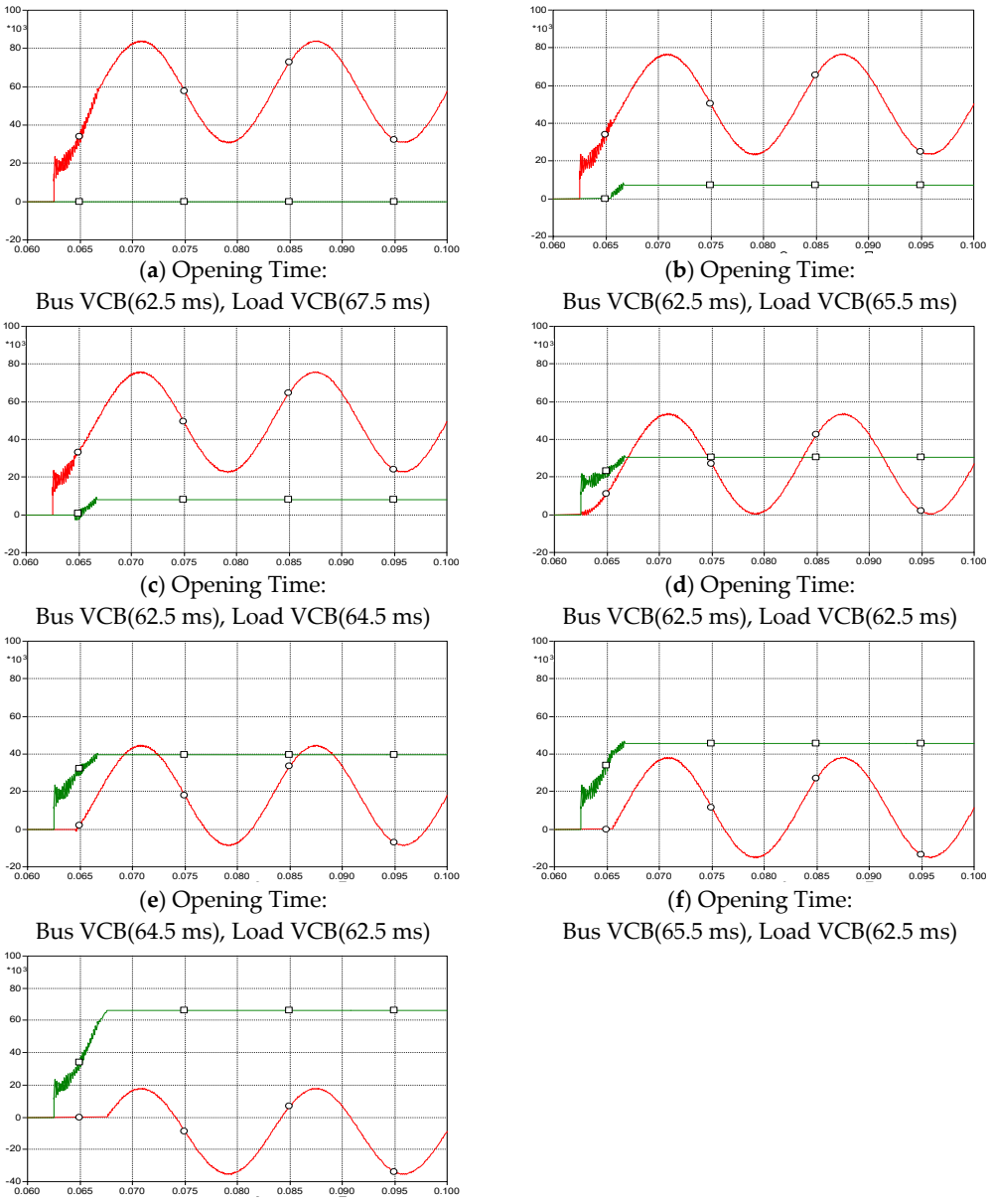

(**a**) Opening Time: Bus VCB(62.5 ms), Load VCB(67.5 ms)

(**b**) Opening Time: Bus VCB(62.5 ms), Load VCB(65.5 ms)

(**c**) Opening Time: Bus VCB(62.5 ms), Load VCB(64.5 ms)

(**d**) Opening Time: Bus VCB(62.5 ms), Load VCB(62.5 ms)

(**e**) Opening Time: Bus VCB(64.5 ms), Load VCB(62.5 ms)

(**f**) Opening Time: Bus VCB(65.5 ms), Load VCB(62.5 ms)

(**g**) Opening Time: Bus VCB(67.5 ms), Load VCB(62.5 ms)

Figure 15. Simulation results of the transient recovery voltage for the proposed method.

Table 5. Transient recovery voltage for the switchboard with a double circuit breaker structure.

Opening Time (ms)			TRV (kV)		Waveforms
Bus VCB (Upper Breaker)	**Load VCB (Lower Breaker)**	**Delta T**	**Bus VCB**	**Load VCB**	
62.5	67.5	−5.0	84.1	0.0	Figure 15a
62.5	65.5	−3.0	76.8	8.5	Figure 15b
62.5	64.5	−2.0	76.0	9.3	Figure 15c
62.5	62.5	0.0	53.7	31.5	Figure 15d
64.5	62.5	2.0	44.7	40.5	Figure 15e
65.5	62.5	3.0	38.3	46.9	Figure 15f
67.5	62.5	5.0	35.4	66.1	Figure 15g

4. Conclusions

This paper addressed the difference between the capacitor bank and the harmonic filter bank and analyzed the transient characteristics during back-to-back switching. The cause of the differences between these banks was found to be caused by design, taking into account L and C.

The switching transients of the filter banks are described by the analytical approach and field measurements for 150 MVA back-to-back filter banks were provided to support the switching phenomena described in the paper. In the case of the filter banks, a lower back-to-back inrush current and higher transient recovery voltage compared to capacitor banks appeared. Therefore, a mitigation method for the transient recovery voltage was needed. To mitigate the high transient recovery voltage, a double-breaker type switchgear was analyzed in terms of the operating sequence and the time of the upper- and lower-breakers. According to the analyses, the effectiveness of the proposed scheme, the optimum sequence, and the operation time was verified to avoid the insulation failure of the breaker during the interruption, by mitigating the transient recovery voltage across each breaker. The proposed method could be a useful guide for back-to-back filter bank switching issues.

Author Contributions: Conceptualization, J.-H.K.; methodology, J.-H.K.; supervision, J.-O.K.; writing (original draft), J.-H.K.; writing (review and editing), J.-H.K. and J.-O.K. All authors have read and agreed to the published version of the manuscript.

Funding: This research received no external funding.

Conflicts of Interest: The authors declare no conflict of interest.

References

1. Dolara, A.; Leva, S. Power Quality and Harmonic Analysis of End User Devices. *Energies* **2012**, *5*, 5453–5466. [CrossRef]
2. Phannil, N.; Jettanasen, C.; Ngaopitakkul, A. Harmonics and Reduction of Energy Consumption in Lighting Systems by Using LED Lamps. *Energies* **2018**, *11*, 3169. [CrossRef]
3. Nassif, A.B.; Xu, W.; Freitas, W. An Investigation on the Selection of Filter Topologies for Passive Filter Applications. *IEEE Trans. Power Deliv.* **2009**, *24*, 1710–1718. [CrossRef]
4. Beres, R.N.; Wang, X.; Blaabjerg, F.; Liserre, M.; Bak, C.L. Optimal Design of High-Order Passive-Damped Filtersfor Grid-Connected Applications. *IEEE Trans. Power Electron.* **2016**, *31*, 2083–2098. [CrossRef]
5. Zhang, G.; Wang, Y.; Xu, W.; Sitther, E. Characteristic Parameter-Based Detuned C-Type Filter Design. *IEEE Power Energy Technol. Syst. J.* **2018**, *5*, 65–72. [CrossRef]
6. Cano-Plata, E.A.; Ustariz-Farfan, A.J.; Soto-Marin, O.J. Electric Arc Furnace Model in Distribution Systems. *IEEE Trans. Ind. Appl.* **2015**, *51*, 4313–4320. [CrossRef]
7. Acha, E.; Semlyen, A.; Rajakovic, N. A harmonic domain computational package for nonlinear problems and its application to electric arcs. *IEEE Trans. Power Deliv.* **1990**, *5*, 1390–1397. [CrossRef]
8. Alonso, M.A.P.; Donsion, M.P. An improved time domain arc furnace model for harmonic analysis. *IEEE Trans. Power Deliv.* **2004**, *19*, 367–373. [CrossRef]

9. Salgado-Herrera, N.M.; Campos-Gaona, D.; Anaya-Lara, O.; Robles, M.; Rodríguez-Hernández, O.; Rodríguez-Rodríguez, J.R. THD Reductionin Distributed Renewables Energy Accessthrough Wind Energy Conversion System Integration under Wind Speed Conditionsin Tamaulipas, Mexico. *Energies* **2019**, *12*, 3550. [CrossRef]
10. Xu, H.; Shao, Z.; Chen, F. Data-Driven Compartmental Modeling Methodfor Harmonic Analysis—A Study of the Electric Arc Furnace. *Energies* **2019**, *12*, 4378. [CrossRef]
11. Mendis, S.R.; Gonzalez, D.A. Harmonic and transient overvoltage analyses in arc furnace power systems. *IEEE Trans. Ind. Appl.* **1992**, *28*, 336–342. [CrossRef]
12. Smith, L.M. A practical approach in substation capacitor bank applications to calculating, limiting, and reducing the effects of transient currents. *IEEE Trans. Ind. Appl.* **1995**, *31*, 721–724. [CrossRef]
13. Padimiti, D.S.; Christian, M.B.; Jarvinen, J. Effective Transient-Free Capacitor Switching (TFCS) for Large Motor Starting on MV Systems. *IEEE Trans. Ind. Appl.* **2019**, *55*, 1012–1020. [CrossRef]
14. Mysore, P.G.; Mork, B.A.; Bahirat, H.J. Improved Application of Surge Capacitors for TRV Reduction When Clearing Capacitor Bank Faults. *IEEE Trans. Power Deliv.* **2010**, *25*, 2489–2495. [CrossRef]
15. Ghanbari, T.; Farjah, E.; Zandnia, A. Solid-state transient limiter for capacitor bank switching transients. *IET Gener. Transm. Distrib.* **2013**, *7*, 1272–1277. [CrossRef]
16. Badrzadeh, B. Transient Recovery Voltages Caused by Capacitor Switching in Wind Power Plants. *IEEE Trans. Ind. Appl.* **2013**, *49*, 2810–2819. [CrossRef]
17. Dionise, T.J.; Lorch, V.; Brazil, B.J. Power Quality Investigation of Back-to-Back Harmonic Filters for a High-Voltage Anode Foil Manufacturing Facility. *IEEE Trans. Ind. Appl.* **2010**, *46*, 694–702. [CrossRef]
18. Kuczek, T.; Florkowski, M.; Piasecki, W. Transformer Switching with Vacuum Circuit Breaker: Case Study of PV Inverter LC Filters Impacton Transient Overvoltages. *IEEE Trans. Power Deliv.* **2016**, *31*, 44–49. [CrossRef]
19. Dudley, R.F.; Fellers, C.L.; Bonner, J.A. Special design considerations for filter banks in arc furnace installations. *IEEE Trans. Ind. Appl.* **1997**, *33*, 226–233. [CrossRef]
20. Spurling, K.L.; Poitras, A.E.; McGranaghan, M.F.; Shaw, J.H. Analysis and Operating Experience for Back-to-Back 115 KV Capacitor Banks. *IEEE Trans. Power Deliv.* **1987**, *2*, 1255–1263. [CrossRef]
21. Furumasu, B.C.; Hasibar, R.M. Design and installation of 500 kV back-to-back shunt capacitor banks. *IEEE Trans. Power Deliv.* **1992**, *7*, 539–545. [CrossRef]
22. Zhang, Y.; Yang, H.; Wang, J.; Geng, Y.; Liu, Z.; Jin, L.; Yu, L. Influence of High-Frequency High-Voltage Impulse Conditioning on Back-to-Back Capacitor Bank Switching Performance of Vacuum Interrupters. *IEEE Trans. Plasma Sci.* **2016**, *44*, 321–330. [CrossRef]
23. Kalyuzhny, A. Switching Capacitor Bank Back-to-Back to Underground Cables. *IEEE Trans. Power Deliv.* **2013**, *28*, 1128–1137. [CrossRef]
24. Patcharoen, T.; Ngaopitakkul, A. Transient inrush current detection and classification in 230 kV shunt capacitor bank switching under various transient-mitigation methods based on discrete wavelet transform. *IET Gener. Transm. Distrib.* **2018**, *12*, 3718–3725. [CrossRef]
25. Srisongkram, W.; Fuangpian, P.; Suwanasri, T.; Suwanasri, C. Investigationon Dielectric Failure of High Voltage Equipmentin Substation Caused by Capacitor Bank Switching. *J. Electr. Eng. Technol.* **2019**, *14*, 849–860. [CrossRef]
26. Das, J.C. *Power System Harmonics and Passive Filter Designs*; John Wiley & Sons: Hoboken, NJ, USA, 2015.
27. IEEE Std C37.012-2014. *IEEE Guide for Application of Capacitance Current Switching for AC High-Voltage Circuit Breakers Above 1000 V*; IEEE: Piscataway, NJ, USA, 2014.
28. IEEE Std 1531-2003. *IEEE Guide for Application and Specification of Harmonic Filters*; IEEE: Piscataway, NJ, USA, 2003.
29. IEEE Std 1036-2010. *IEEE Guide for the Application of Shunt Power Capacitors*; IEEE: Piscataway, NJ, USA, 2011.
30. Greenwood, A. *Electrical Transients in Power Systems*; John Wiley & Sons: Hoboken, NJ, USA, 1971.